Manuscript Details

Manuscript number	JAG_2019_22
Title	Estimating above ground biomass as an indicator of carbon storage in vegetated wetlands of the grassland biome of South Africa
Article type	Research Paper

Abstract

Wetlands store higher carbon content relative to other terrestrial ecosystems, despite the small extent they occupy. The increase in temperature and changes in rainfall pattern may negatively affect their extent and condition, and thus the process of carbon accumulation in wetlands. The introduction of the Sentinel series (S1 and S2) and WorldView space-borne sensors have enabled monitoring of herbaceous above ground biomass (AGB) in small and narrow wetlands in semi-arid area. The objective of this study was to assess (i) the capabilities of the high to moderate resolution sensors in estimating herbaceous AGB of vegetated wetlands and (ii) whether significant differences exists between the AGB ranges of wetland and surrounding dryland vegetation. WorldView-3 (WV3) yielded the highest AGB prediction accuracies (R2 = 0.63 and RMSE = 169.28 g/m2) regardless of the incorporation of bands only, indices only or the combination of bands and indices. In general, the optical sensors yielded higher modelling accuracies (improvement in R2 of 0.04-0.07 and RMSE of 11.48-17.28 g/m2) than the single Synthetic Aperture Radar (SAR) sensor but this was marginal depending on the scenario. Incorporating Sentinel 1A (S1) dual polarisation channels and Sentinel 2A (S2) reflectance bands, in particular, yielded higher accuracies (improvement in R2 of 0.03-0.04 and RMSE of 5.4-16.88 g/m2) than the use of individual sensors alone and was also equivalent to the performance of the high resolution WV3 sensor results. Wetlands had significantly higher AGB compared to the surrounding terrestrial grassland (with a mean of about 80 g/m2 more). Monitoring herbaceous AGB at the scale of the wetland extent in semi-arid to arid grassland enables improved understanding of their carbon sequestration potential and serves as a proxy for functional intactness.

Keywords	Vegetation biomass; AGB; wetland types; carbon sequestration; remote sensing; earth observation; Sentinel sensors
Taxonomy	Data Modelling, Multi-Imaging, Mapping

Corresponding Author	Laven Naidoo
Corresponding Author's Institution	Council for Scientific and Industrial Research
Order of Authors	Laven Naidoo, Heidi van Deventer, Abel Ramoelo, Renaud Mathieu, Basanda Nondlazi, Ridhwannah Gangat

Suggested reviewers	Moses Cho, xinyue ye, Thuy Le Toan, ELhadi Adam

Submission Files Included in this PDF

File Name [File Type]

LNaidoo_Cover_Letter_JAEG.docx [Cover Letter]

20181220_WRC_K5 2545 FINAL_DRAFT_Shortened.pdf [Manuscript File]

To view all the submission files, including those not included in the PDF, click on the manuscript title on your EVISE Homepage, then click 'Download zip file'.

Research Data Related to this Submission

There are no linked research data sets for this submission. The following reason is given:
Data will be made available on request

Laven Naidoo
CSIR – NRE
P.O.Box 395
Pretoria
0001
South Africa

Dr. F. van der Meer
Editor-in-Chief
Faculty of Geo-Information Science and Earth Observation
University of Twente, Enschede
Netherlands

Re: Submission of manuscript for peer-review

Dear Sir

I would like to submit a full paper entitled "Estimating above ground biomass as an indicator of carbon storage in vegetated wetlands of the grassland biome of South Africa" to the *International Journal of Applied Earth Observation and Geoinformation*. The objective was to assess the capabilities of the high (WorldView-3) to moderate resolution (Sentinel-1/2) sensors in estimating herbaceous above ground biomass (AGB) of vegetated wetlands. Wetlands store higher carbon content relative to other terrestrial ecosystems, despite the small extent they occupy. The accumulation of organic carbon in these small and narrow systems, however, is threatened by land transformation, alteration of the hydrological regime and disturbances (e.g. grazing and fire). Comparing a series of moderate resolution, freely available sensors (e.g. Sentinel 1 and 2) to high resolution WorldView-3 imagery would shine some light on the applicability of such sensors in the monitoring of these wetlands systems. The authors believe that this study improved upon the current abilities to monitor palustrine wetland vegetation AGB in the grassland biome of South Africa.

I hope you find that this paper meets the required standards for publication.

Contact details of the corresponding Author, Laven Naidoo:
Email lnaidoo@csir.co.za
Address: *same as above*
Tel: +27 12 842 7242 or
Fax: +27 12 841 3909

Kind regards
Laven Naidoo

Estimating above ground biomass as an indicator of carbon storage in vegetated wetlands of the grassland biome of South Africa

Authors:

Laven Naidoo[a], Heidi van Deventer[a,b], Abel Ramoelo[c,e], Renaud Mathieu[a,d], Basanda Nondlazi[a], Ridhwannah Gangat[b]

[a] *Council for Scientific and Industrial Research (CSIR), Ecosystem Earth Observation, Pretoria, South Africa*

[b] *University of the Witwatersrand, School of Geography, Archaeology and Environmental Studies, Private Bag 3, WITS 2050, South Africa*

[c] *University of Limpopo, Risk and Vulnerability Assessment Centre, Sovenga, Limpopo, Private Bag X1106, Polokwane 0727, South Africa*

[d] *University of Pretoria, Department of Geography, Geoinformatics and Meteorology, Private BagX20, Hatfield 0028, South Africa*

[e] *Scientific Services, South African National Parks, P.O. Box 787, Pretoria 0001, South Africa*

Author e-mail addresses:

LNaidoo@csir.co.za, HvDeventer@csir.co.za, abel.ramoelo@sanparks.org, RMathieu@csir.co.za, BNondlazi@csir.co.za, ridwanagangat@gmail.com

Corresponding author:

Laven Naidoo

Council for Scientific and Industrial Research (CSIR), P.O. Box 395, Pretoria 0001, South Africa

Tel: +27 12 842 7242

Fax: +27 12 841 3909

E-mail: LNaidoo@csir.co.za

Abstract

Wetlands store higher carbon content relative to other terrestrial ecosystems, despite the small extent they occupy. The increase in temperature and changes in rainfall pattern may negatively affect their extent and condition, and thus the process of carbon accumulation in wetlands. The introduction of the Sentinel series (S1 and S2) and WorldView space-borne sensors have enabled monitoring of herbaceous above ground biomass (AGB) in small and narrow wetlands in semi-arid area. The objective of this study was to assess (i) the capabilities of the high to moderate resolution sensors in estimating herbaceous AGB of vegetated wetlands and (ii) whether significant differences exists between the AGB ranges of wetland and surrounding dryland vegetation. WorldView-3 (WV3) yielded the highest AGB prediction accuracies (R^2 = 0.63 and RMSE = 169.28 g/m^2) regardless of the incorporation of bands only, indices only or the combination of bands and indices. In general, the optical sensors yielded higher modelling accuracies (improvement in R^2 of 0.04-0.07 and RMSE of 11.48-17.28 g/m^2) than the single Synthetic Aperture Radar (SAR) sensor but this was marginal depending on the scenario. Incorporating Sentinel 1A (S1) dual polarisation channels and Sentinel 2A (S2) reflectance bands, in particular, yielded higher accuracies (improvement in R^2 of 0.03-0.04 and RMSE of 5.4-16.88 g/m^2) than the use of individual sensors alone and was also equivalent to the performance of the high resolution WV3 sensor results. Wetlands had significantly higher AGB compared to the surrounding terrestrial grassland (with a mean of about 80 g/m^2 more). Monitoring herbaceous AGB at the scale of the wetland extent in semi-arid to arid grassland enables improved understanding of their carbon sequestration potential and serves as a proxy for functional intactness.

Keywords

Vegetation biomass, AGB, wetland types, carbon sequestration, remote sensing, earth observation, Sentinel sensors

1. Introduction

The above ground biomass (AGB) of wetland vegetation contributes to peat formation and subsequently to carbon sequestration. The inundation of wetlands favours carbon sequestration, while a number of biotic, thermal and chemical processes, as well as the intactness of the wetland and vegetation types can increase the rate of accumulation (Amundson, 2001; Nahlink and Fennessy, 2016). Despite the small extent of wetlands (estimated at 5-8%), it is estimated that they store a higher carbon content relative to other terrestrial ecosystems (Amthor et al., 1998; Kayranli et al., 2010; Mitsch and Gosselink, 2015). A number of threats prohibit this continuous process of organic carbon accumulation, including land transformation to urban, cropland or forestry, alteration of the hydrological regime of wetlands, continuous grazing or fire regimes (Jones and Donnelly, 2004; Kayranli et al., 2010). The increasing temperatures observed and predicted for climate change, as well as the associated increase in evapotransporation and changing rainfall patterns, may exacerbate current pressures (Poiani et al., 1995; Jones and Donnelly, 2004; IPCC, 2013; MacKellar et al., 2014; Van Wilgen et al., 2016). To facilitate the monitoring of the process of AGB accumulation in palustrine wetlands and adjacent grasslands, frequent temporal monitoring at a regional scale is required.

Traditional assessments of herbaceous AGB in wetland are a tedious procedure, requiring *in situ* samples across various and often inaccessible terrains. AGB measured in the field ranged from 30 to 1 720 g/m², depending on the hydrogeomorphic wetland type, climatic region and vegetation growth, as reviewed by Truus (2011). Grasses and sedges AGB (dry weight) showed ranges between 30 – 200 g/m², whereas macrophytes such as *Phragmites* species AGB ranged from 300 to 1300 g/m² (Truus, 2011). More information, however, is required for palustrine wetlands, located in semi-arid regions of the southern hemisphere. Destructive methods of quantifying grass AGB are, however, time consuming and costly and are often limited to a number of sites. In wetlands physical measurement of AGB is also strongly limited due to issues of manoeuvrability and access due to the presence of water. Remote sensing technology, in contrast, has established non-destructive methods for estimating total biomass and the carbon stock in vegetation at a regional scale and in inaccessible areas (Liao et al., 2013).

Regional estimation of AGB with remote sensing has mostly been done in the terrestrial environment, with limited studies focusing on wetland vegetation. For the large Poyang Lake system in China, Synthetic Aperture Radar (SAR) and optical systems were able to estimate the AGB of wetland vegetation with coefficients of determination (R^2) above 0.70 and Root Mean Square Errors (RMSEs) below 140 g/m^2 (Liao et al., 2013; Li & Liu, 2002). Also in China but Inner Mongolia, Xie et al., (2009) utilised empirical models, derived from optical Landsat data, to obtain mean ranges of grass AGB of up to 147g/m^2. In South Africa, the AGB of a Papyrus (alien) dominated wetland has been estimated with WorldView-2 which achieved accuracies

of R^2 of 0.76 and RMSE of 442 g/m^2 with a predicted AGB range of 2000 to 5000 g/m^2 (Mutanga et al., 2012).

The use of vegetation indices and the red-edge band of newer optical sensors have improved the estimation of wetland and terrestrial AGB, overcoming the saturation effect of higher AGB and dense canopies (Penuelas et al., 1993; Mutanga et al., 2012; Ramoelo et al., 2015; Sibanda et al., 2017). In grasslands, vegetation indices offer the advantage of superseding the influences of soil background, atmospheric composition and the viewing and zenith angle effects while enhancing the vegetation signal, when estimating AGB. Leaf Area Index (LAI), i.e. the half of the total green leaf area per unit area (Reid and Huq, 2005), is an index which captures the energy interactions between the leaves and the environment. LAI serves as a good indicator of vegetation growth and productivity and is also considered in the literature as proxy to AGB (Fan et al., 2009; Van Wijk and Williams, 2005; Masemola et al., 2014). Microwave radar (e.g. Synthetic Aperture Radar - SAR) technologies, on the other hand, is often favoured above optical sensors because of its cloud-penetrating capacities. However, the differential scattering of radar signal under inundated or non-inundated scenarios in wetlands can result in errors in the estimation of wetland biomass (Silva et al., 2008; Liao et al., 2013; Gallant, 2015). The integration of optical and SAR technologies have also been proven to be more accurate than the individual technologies separately (Huang et al., 2016). Using these combined datasets, the study documented an improvement in RMSE of ~300 g/m^2 compared to the best individual sensor scenario (in this case Terra ASTER and ERS-2 SAR). To date, however, most SAR and optical sensors used for estimating herbaceous AGB were coarse resolution sensors, with spatial resolutions of >30 m. In semi-arid

122 regions, however, the extent of wetlands is often smaller in diameter and therefore
123 requires finer spatial resolutions.

124

125 The availability of newer Earth Observation satellites such as the European Space
126 Agency (ESA) Sentinel series, which are now freely available and operational since
127 2015, offers new opportunities to assess the capabilities of determining AGB of
128 palustrine wetland in temperate and semi-arid grasslands. The Sentinel 1A (S1A)
129 satellite hosts a C-band (5.6cm) SAR sensor operating with various cross and co-
130 polarisation configurations depending on the sensing mode (Vertical-Horizontal or
131 VH, Horizontal-Horizontal or HH, and Vertical-Vertical or VV). Volumetric backscatter
132 interactions, from VH polarised data, and/or the use of co-polarised data (e.g. VV) for
133 double bounce interactions with pole-like plants of the genus Phragmites (as the
134 case in Ye et al., 2010), can allow SAR sensors to be effective for ascertaining
135 vegetation AGB but are restricted from sensing submerged aquatic vegetation due to
136 its inability to penetrate into the water column (Silva et al., 2008). The Sentinel 2A
137 and 2B (S2A; S2B) optical sensors hosts a number of bands in the red-edge region
138 of the electromagnetic spectrum, which has previously shown to produce more
139 accurate vegetation biomass estimates (Mutanga et al., 2012; Sibanda et al., 2015).
140 The S2A and S2B sensors also offers a spatial resolution of between 10 and 20 m,
141 which may be better suited for the detection of the extent of wetlands in arid and
142 semi-arid regions, compared to the previous sensors. The WorldView 3 (WV3)
143 space-borne sensor (DigitalGlobe Pty Ltd) is also a space-borne sensor which offers
144 a band in the red-edge region but with a spatial resolution below 1 m, however, it is
145 costly to acquire at the regional scale. It remains to be assessed whether these
146 sensors can determine grass AGB across dryland and wetland areas and whether

147 the AGB modelling accuracies between free data platforms (e.g. Sentinel series) and
148 the high resolution state-of-the-art sensor (e.g. WV3) are comparable. The latter is
149 yet to be tested in academic literature from a wetland grass biomass perspective.
150
151 This study, thus, aimed to assess the performance of the S1, S2, and WV3 sensors,
152 together with the addition of LAI as an additional modelling parameter, for estimating
153 herbaceous AGB for both wetlands and surrounding drylands using spectral data
154 and selected established indices. In particular, we (i) compared the ability of radar
155 (S1A) and optical (S2A, WV3) sensors for estimating AGB of vegetated wetlands,
156 separately and combined and (ii) assessed whether significant differences exists
157 between the AGB ranges of wetland and dryland vegetation.
158
159 # 2. Methods
160 ## *2.1. Study area*
161 Approximately 26% of South Africa's surface area is dominated by the grassland
162 biome where a variety of palustrine and lacustrine wetlands occur (Mucina &
163 Rutherford, 2006). The grassland biome is one of the most threatened biomes in
164 South Africa with 45% of it being transformed through expansions in agriculture,
165 plantations, mining and alien plant species (Fourie et al., 2015). Wetlands,
166 particularly in such a biome, are extremely fragmented ecosystems and are also the
167 most endangered ecosystem types in South Africa (Burgoyne et al., 2000). The
168 South African National Water Act, Act 36 of 1998, defines a wetland as 'land which is
169 transitional between terrestrial and aquatic systems where the water table is usually

at or near the surface, or the land is periodically covered with shallow water, and which land in normal circumstances supports or would support vegetation typically adapted to life in saturated soil.' (RSA, 1998). Two study areas, found in the grassland montane areas of South Africa, were chosen: Hogsback and Tevredenpan. The Hogsback study area is located within one of 22 Strategic Water Source Areas of South Africa where rainfall runoff is high and which disproportionally contributes to national water security (Le Maitre et al., 2018). The Tevredenpan study area forms part of the Chrissiesmeer Protected Environment, and owing to the large density of shallow inland depressions, amongst other criteria, qualifies for Ramsar listing (MTPA, 2014).

The Hogsback study area (32.55°S, 26.97°E) is located in montane grasslands of the Amathole mountain range in the Eastern Cape Province (Figure 1A, B). The latter receives between 611 and 1 239 mm rainfall per annum and experience mean annual evapotranspiration of around 1 650 mm (Middleton and Bailey, 2008). The wetland types (Figure 2B) range from valley-bottom and floodplains on lower grassland slopes to seeps on the higher slopes of the mountains, extending to areas between forest plantations of Pine and Eucalyptus species. *Carex acutiformis* forms dominant stands in the low-lying wetlands, with small intermittent patches of *Phragmites australis*. On the higher slopes a greater diversity of grass and sedge communities exist (Janks, 2014). Grazing dominates the land use with cropland, such as maize and soya, providing fodder. Forest plantations are situated to the south of the study area (Figure 1A, B).

194 The Tevredenpan study area (26°12’40.7”S; 30°12’42.6”E) is located in the gradually
195 undulating plateau of South Africa in the grassland biome (Figure 1A, C). It forms
196 part of the largest pan belt in southern Africa (Goudie and Wells, 1995). The Mean
197 Annual Precipitation (MAP) is around 750 mm and the mean annual
198 evapotranspiration is between 1 700 and 1 800 mm per annum (Middleton and
199 Bailey, 2008) while the mean annual temperature ranges from 12.4°C to 25.2°C
200 (Schulze, 1997). Wetlands in the Tevredenpan study area feed two river systems,
201 the Mpuluzi River in the north, and the Pearl stream in the south. A large limnetic
202 and *Phr. australis*-dominated depression, called “Tevredenpan” is located in the
203 western edge of the study area (Figure 2A) with floating macrophytes and a
204 substrate of peatlands (Grundling et al., 2003). A large part of the soil in the valley-
205 bottoms is permanently saturated, though not inundated, whereas valley-bottom and
206 seep wetlands on slopes are seasonally to temporary saturated. A wide variety of
207 grass and sedge species dominate all wetlands (Sieben et al. 2014; Linström 2014),
208 though monotype *Typha capensis*, *Phragmites australis and Carex acutiformis* has
209 been observed for patches in the valley-bottom and river systems.

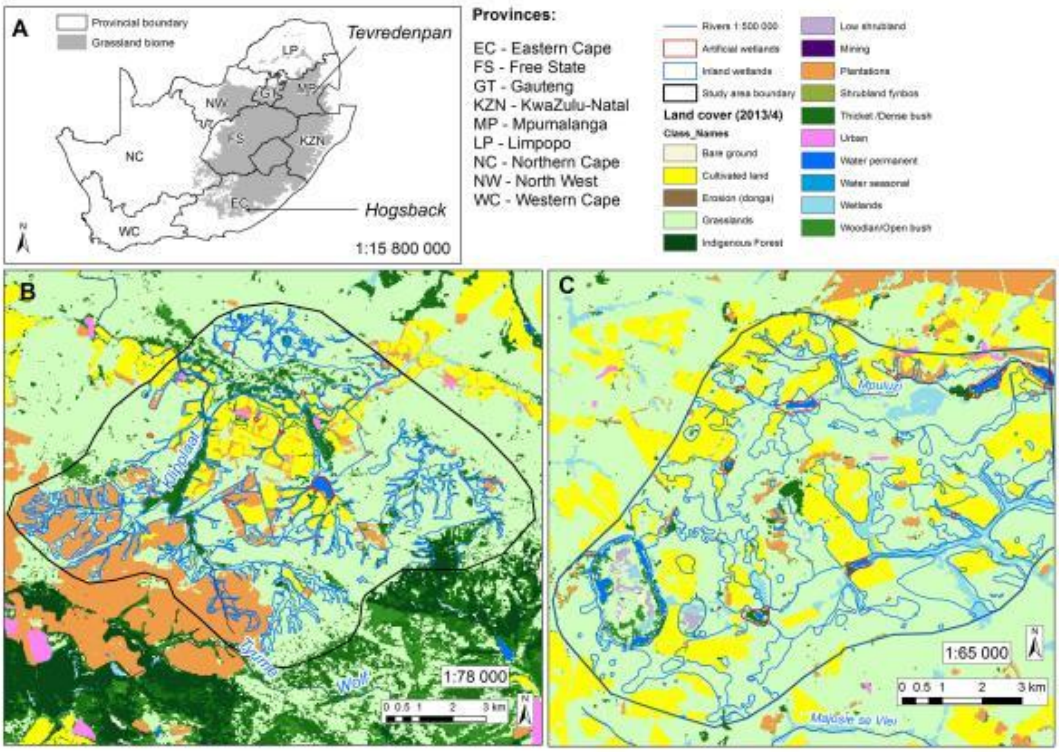

Figure 1: A) The location of the two study areas in the montane grassland biome (grey) of South Africa. B= Land cover classes for the Hogsback study area; C= Land cover classes for the Tevredenpan study area (GeoTerraImage, GTI Pty Ltd. 2015)

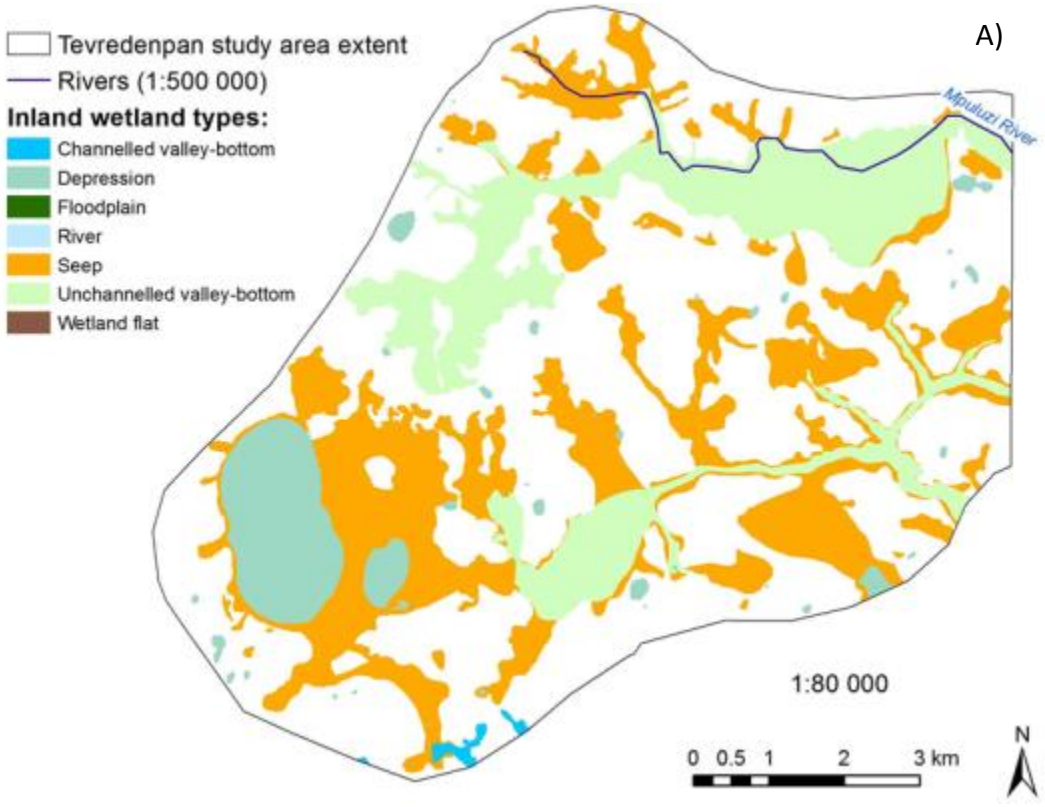

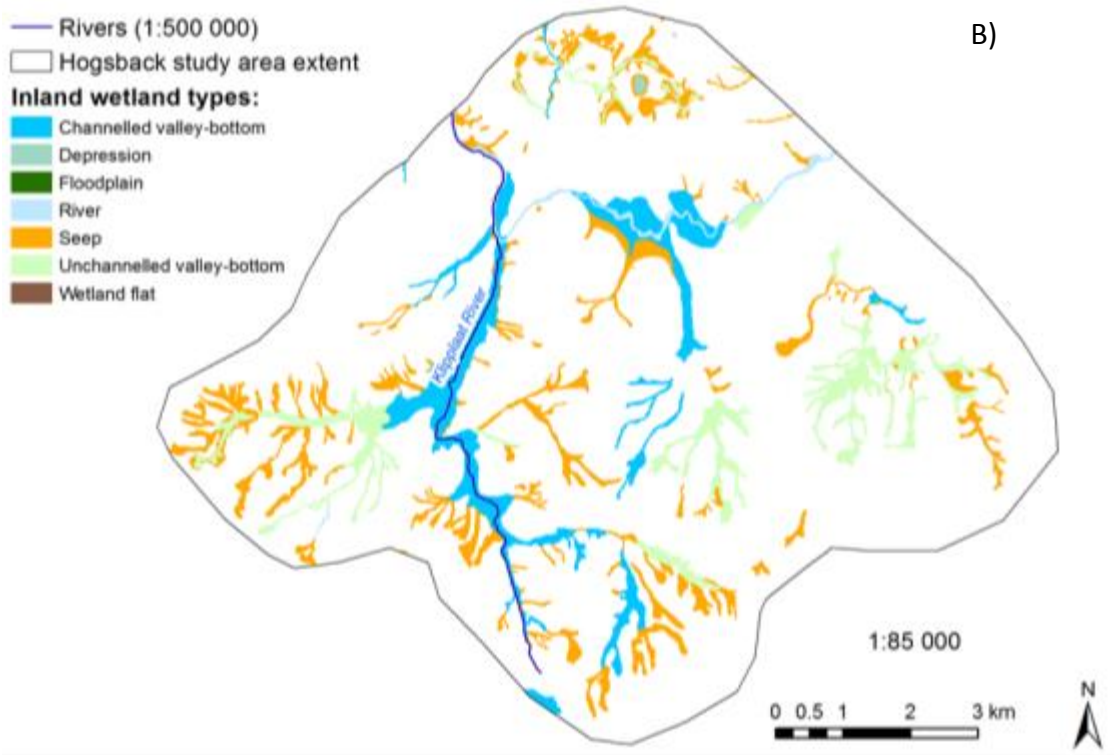

Figure 2: Hydrogeomorphic wetland types for the (A) Tevredenpan study area and (B) Hogsback study area.

Hydrogeomorphic (HGM) wetland types have been captured according to South Africa's tiered Classification System (National Wetlands Map 5; Van Deventer et al., submitted) for inland wetlands which distinguished five HGM wetland types, namely channelled valley-bottom (CVB), unchannelled valley-bottom (UVB), depression, floodplain, seep and wetland flat wetlands (Ollis et al., 2015). This classification system was applied for both sites. Features inside the HGM wetland type boundaries were considered to be wetlands while features outside were considered to be drylands.

2.2. Data collection

Ground Range Detected (GRD) images of the Sentinel-1A C-band sensor, in Interferometric Wide (IW) swath mode, were acquired from the Alaska Satellite

231 Facility (ASF) (https://www.asf.alaska.edu/sentinel/data/). SAR imagery was
232 acquired in the transitional seasons (spring and autumn) to allow the growth and
233 accumulation of wetland vegetation biomass (both wetland and dryland) which can
234 be sensed by the SAR sensor while avoiding the summer season where the bulk of
235 the rainfall would negatively impact the backscatter. Images of the Sentinel-2A
236 Multi-spectral Instrument (MSI) were downloaded from the
237 https://remotepixel.ca/projects/satellitesearch.html website, and the WV3 images
238 were purchased from DigitalGlobe Pty Ltd (Table 1). The S2 and WW3 images were
239 selected with <10% clouds at the middle to end of the peak of the hydroperiod in the
240 grassland (i.e. summer to late summer), except for one S2A acquired during the late
241 winter due to cloud presence of earlier scenes. During this period, it is the end of the
242 growing season of the sedges and grasses which means that there is optimal
243 greenness with limited water inundation.

244 **Table 1: Space-borne images accessed for the two study areas in South Africa**

Study Area	Sensor	Final spatial resolution	Image data	Season
Tevredenpan	S1A	20m	12/04/2017	Autumn
	S2A	10m	19/01/2017	Summer
	WV3	1m	21/03/2017	Summer
Hogsback	S1A	20m	21/09/2016	Spring
	S2A	10m	24/08/2016	Winter
	WV3	1m	21/03/2017	Summer

245 **S1A = Sentinel-1A, S2A =Sentinel-2A, WV3 = WorldView-3*

246

247 ## *2.3. Image and data pre-processing*

248 The S1A GRD intensity datasets were processed in GAMMA (TM) SAR pre-
249 processing software. The datasets were subjected to the following steps: combining
250 of Sentinel-1A bursts, multi-looking, radiometric calibration (from digital numbers to
251 sigma nought backscatter), geocoding and topographic normalization. In order to

252 reduce typical SAR speckle, multi-looking factors of 2 and 2 were applied to the
253 range and azimuth directions, respectively. The Shuttle Radar Topography Mapper
254 (SRTM) Digital Elevation Model (DEM) at 30 m pixel size (SRTM 30) was used for
255 geocoding and topographic normalization. The Sentinel-1 images were processed to
256 a final spatial resolution of 20m. Sentinel-2 images were acquired at the 1C
257 processing level which included orthorectification as a pre-processing step. The
258 Sen2Cor algorithm, available through the ESA's Sentinel Application Platform
259 (SNAP), were used to atmospherically correct the multispectral Sentinel-2A images.
260 The algorithm parameter were chosen based on the location and environment type
261 of the study sites as well as the values recommended in the Sen2Cor configuration
262 and user manual (Mueller-Wilm, 2017).
263

264 ### *2.4. Field AGB and LAI sampling*

265 Field visits were made to the study sites in November 2016 for Hogsback and in
266 March 2017 for Tevredenpan for the collection of wet AGB and LAI data for 62
267 sample plots (30 sites from Hogsback and 32 from Tevredenpan). We selected
268 6X6m sample plots within homogeneous patches (generally bigger than 20X20m to
269 take into account the pixel size of Sentinel 1) in terms of dominant species
270 composition and general grass structure (height, cover and AGB). These plots
271 prioritised the capturing of the representative range of AGB. A differentially
272 corrected GPS location (less than 50cm horizontal error using a Trimble GEO 7X
273 GPS) was acquired from the centre point of each sample plot. Within each sample
274 plot, three 0.5X0.5m quadrants were randomly placed from which wet herbaceous
275 AGB was harvested, weighed, and subsequently averaged over the entire sample
276 plot. Also within each 0.5X0.5m quadrant, three leaf area index (LAI) measurements

were taken from the LiCOR LAI-2200C Plant Canopy Analyzer which were also averaged over the entire sample plot. The plot level LAI measurements were then utilised as an additional independent variable in the modelling procedure (motivated for in section 2.6). LAI was also considered in the literature as proxy to AGB (Fan et al., 2009; Van Wijk and Williams, 2005). The wet herbaceous AGB was subsequently dried in an oven at 80°C until the weight stabilised (i.e. no change in weight over a 48 hour period) to get dry AGB measurements which were used as the dependent variable in the modelling procedure.

2.5. Extraction of remote sensing data and computation of vegetation indices and regional LAI

For the extraction of the remote sensing predictors or independent variables, the 62 sample plot 6X6m polygons and point shapefiles (centred over the GPS locations) were used depending on the spatial resolution of the remote sensing datasets. The 62 sample plot points were used to extract a single pixel value of S1A (backscatter) and S2A (reflectance band values) while the 62 sample plot 6X6m polygons were used to extract the mean reflectance band values from WV3.

The presence of free running or standing water in wetlands does alter the overall spectral signal in optical sensors as water absorbs electromagnetic radiation. Despite this fact, particular spectral regions such as the green region, with greater light penetration in water (Kirk, 1994) and the NIR and red- edge regions (Mutanga et al., 2012) have been proven useful in studying submerged and non-submerged wetland vegetation. These spectral regions can be combined in the form of VIs and

band ratios which have been proven to correlate highly with wetland vegetation biomass (Huang et al., 2016, Adam et al., 2010, Mutanga et al., 2012). A variety of VIs and band ratios, which were known to correlate well with AGB estimation and vegetation structure, were derived from the reflectance and backscatter polarisation data (Table 2 below).

Table 2: Formulae of Vegetation Indices and band ratios used as model predictor variables

Index	Formula	Sentinel-1	Sentinel-2	WorldView-3
		Bands θ	Bands σ	Bands ß
NDVI Red Edge 1	(NIR -RE)/(NIR+RE)		(B8-B5)/(B8+B5)	
NDVI Red Edge 2	(NIR -RE)/(NIR+RE)		(B8-B6)/(B8+B6)	(B8-B6)/(B8+B6)
NDVI Red Edge 3	(NIR -RE)/(NIR+RE)		(B8-B7)/(B8+B7)	
NDVI Red Edge 4	(NIR -RE)/(NIR+RE)			(B7-B6)/(B7+B6)
NDVI Green 1	(NIR -GR)/(NIR+GR)		(B8-B3)/(B8+B3)	(B8-B3)/(B8+B3)
NDVI Green 2	(NIR -GR)/(NIR+GR)			(B7-B3)/(B7+B3)
Band Ratio 1	NIR/RE		B8/B5	
Band Ratio 2	NIR/RE		B8/B6	B8/B6
Band Ratio 3	NIR/RE		B8/B7	
Band Ratio 4	NIR/RE			B7/B6
Band Ratio 5	NIR/GR		B8/B3	B8/B3
Band Ratio 6	NIR/GR			B7/B3
SAR Band Ratio	VH/VV	B2/B1		

B: band (sensor specific); NIR: Near Infrared; RE: Red Edge; GR: Green; VH and VV: cross and co-polarisations

θ: B2 = VH, B1 = VV; σ: Refer to https://earth.esa.int/web/sentinel/user-guides/sentinel-2-msi/resolutions/spatial for band identities; ß = Refer to http://www.landinfo.com/WorldView3.htm for multispectral band identities

Depending on the number of bands available in each sensor the following summary of derived VIs and band ratios were made. S1A predictor variables included VH and VV backscatter channels and the VH/VV band ratio. S2A predictor variables included 10 reflectance bands, 3 Red Edge and 1 Green band NDVI indices and 4 reflectance band ratios. WV3 predictor variables included 7 reflectance bands, 2 Red Edge and 2 Green band NDVI indices and 4 reflectance band ratios. This resulted in a

316 modelling dataset consisting of 36 remote sensing predictor variables and field
317 based LAI measurements.

318

319 Since field LAI was used as an additional predictor to model AGB the spatial
320 distribution of LAI across both study areas was required to apply the AGB models
321 across the images. The spatial maps of LAI were created by using an LAI PROSAIL
322 radiative transfer model (RTM) (executed in Environment for Visualizing Images
323 Integrative Development Language or ENVI IDL), developed from Darvishzadeh et
324 al. (2008), which was applied to the preferred optical image that emerged from the
325 modelling scenarios. Table 3 below, documents the various environmental variable
326 settings used in this study which was specific for the acquisition data and was
327 parameterised using the LAI range from the ground data.

328 **Table 3: Specific range values of the tuning parameters within the LAI PROSAIL radiative transfer model**

Variable	*Hogsback*		*Tevredenpan*	
	Min	**Max**	**Min**	**Max**
Chlorophyll (µg/cm^2)	0	90	0	90
Leaf Area Index (m^2/m^2)	0	10	0	10
Carotenoid Content (µg/cm^2)	0	25	0	25
Total Brown Pigment (unit less)	0	1	0	1
Equivalent Water Thickness (cm)	0.004	0.04	0.004	0.04
Dry Matter Content (g/cm^2)	0.0019	0.165	0.0019	0.165
Leaf Structure Parameter (N)	1.2 (Mean)	0.3 (Std)	1.2 (Mean)	0.3 (Std)
Average Leaf Angle (°)	25	80	25	80
Hot Spot (m/m)	0.2 (Mean)	0.01 (Std)	0.2 (Mean)	0.01 (Std)
Viewing Zenith Angle (°)	6.2	6.2	7.7	7.7
Solar Zenith Angle (°)	25.25	25.25	28.39	28.39
Rel. Azimuth Angle (°)	153.32	153.32	164.11	164.11
Soil Coefficient (unit less)	0	1	0	1
Note: Diffuse Fraction of 0.70 and default soil reflectance profile 10000 number of Look-up samples and 85 Random Seed				

329

330 ***2.6. Random Forest modelling and modelling scenarios***

A Random Forest (RF) machine learning algorithm was used as the regression approach for this study. The following modelling scenarios (18 in total) were implemented (the number of inputs is listed in parentheses, refer to Table 2):

1) S1 only, 3 scenarios: backscatter (2), SAR band ratio (1) and backscatter + SAR band ratio (3)

2) S2 only, 3 scenarios: reflectance (10), VIs + reflectance band ratios (8) and reflectance + VIs + reflectance band ratios (18)

3) WV3 only, 3 scenarios: reflectance (7), VIs + reflectance band ratios (8) and reflectance + VIs + reflectance band ratios (15)

4) S1 + S2, 3 scenarios: backscatter + reflectance (12), VIs + SAR band ratio + reflectance band ratios (9) and backscatter + reflectance + VIs + SAR band ratio + reflectance band ratios (21)

5) S1 + WV3, 3 scenarios: backscatter + reflectance (9), VIs + SAR band ratio + reflectance band ratios (9) and backscatter + reflectance + VIs + SAR band ratio + reflectance band ratios (18)

6) S2+WV3, 3 scenarios: reflectance (17), VIs + reflectance band ratios (16) and backscatter + reflectance + VIs + reflectance band ratios (33)

RF is widely considered to be more robust than other parametric regression techniques (Naidoo et al., 2014; Ismail and Mutanga, 2010) and have been utilised in similar remote sensing studies of grass biomass estimation (Adam et al, 2014; Mutanga et al., 2012; Ramoelo et al., 2015). Due to the large number of predictor variables a RF-based variable importance selection procedure was conducted, using

354 the ‘caret’ package in R statistical software, to remove highly co-linear variables
355 which likely may cause model overfitting. This process was based on the percentage
356 inclusive mean squared error (%IncMSE), and was implemented for modelling
357 scenarios which required more than 10 predictor variables as inputs. During the
358 variable importance selection process, 100 bootstrapped RF models, which utilised a
359 70% versus 30% split in training and validation datasets, were computed for each
360 scenario and the %IncMSE values of each of the predictor variables were averaged
361 across the 100 iterations and ranked. The ten predictor variables with the highest
362 %IncMSE values were used. For modelling the AGB retrieval, 100 bootstrapped RF
363 models were computed again but using only the top 10 ranked predictor variables.
364 This bootstrapping approach was implemented for added robustness and mean
365 validation accuracy statistics (coefficient of determination or R^2, Root Mean Square
366 Error or RMSE and Standard Error of Prediction or SEP) were recorded to determine
367 the performance of the different modelling scenarios. Preliminary analysis of the
368 different modelling scenarios which included and excluded field based LAI illustrated
369 that the inclusion of LAI markedly improved modelling accuracies (and LAI was the
370 most important input variable from an RF variable importance perspective) and was
371 thus included in all modelling scenarios mentioned above.

372

373 ### *2.7. Above ground biomass mapping*

374 The optimal sensor (or sensor combination) and modelling scenario were chosen for
375 the AGB mapping in both sites, where the R^2 was the highest and RMSE and SEP
376 the lowest. The raster layers of the best model variables, including LAI, were
377 resampled to the common spatial resolution and stacked for the RF mapping

procedure which was conducted in R statistical software using 'raster' and 'rgdal' packages.

To assess differences between the wetlands and drylands, 50 random points were extracted for each class and used to extract AGB map values. Plantations, crop fields, waterbodies and artificial wetlands were excluded to restrict the points to relevant classes, and each point were checked to ensure it doesn't fall on any trees or inundated patches. Differences between the wetlands and drylands were assessed using a Shapiro-Wilk t-test and box plots in the R software (RStudio Inc. v. 0.99.491, 2009-2015, R version 3.2.5. for x64bit). Coefficient of Variation (COV) was also calculated. Differences are reported for each site individually for comparative purposes.

3. Results

3.1. Ability of sensors to estimate AGB of vegetated wetlands

According to Table 4, when scrutinising the individual sensors (S1, S2 and WV3) performance alone, WV3 yielded the highest accuracies regardless of the incorporation of bands only, indices only or the combination of bands and indices. In general the optical sensors yielded higher modelling accuracies than the C-band SAR sensor but this is marginal when examining the obtained SEP values (<1% difference between S1 and S2 but ~6% for WV3, p value of R^2 & RMSE < 0.05). The combination of indices/band ratios and reflectance/polarisations, however, provided

minimal benefits in modelling accuracies with the reflectance/polarisation bands contributing the most over the indices and band ratios.

Table 4: Mean RF validation modelling results (of 100 bootstrapped iterations) for AGB prediction using bands, indices and its combinations of Sentinel-1 (S1), Sentinel-2 (S2) and WorldView-3 (WV3) datasets alone

Scenarios	S1 (SAR)			S2 (optical)			WV3 (high res. optical)		
	R²	*RMSE*	*SEP*	*R²*	*RMSE*	*SEP*	*R²*	*RMSE*	*SEP*
Bands (Reflectance/Backscatter)	0.56	186.56	43.42	0.60	175.08	41.48	0.63	169.28	34.86
Indices (NDVIs/Band ratios)	0.52	192.88	46.38	0.50	195.4	46.26	0.53	184.84	40.90
Bands + Indices*	0.55	182.16	39.79	0.60	178.32	40.69	0.61	176.44	34.03

*Top 10 most important variables (LAI included in all scenarios); RMSE is in g/m^2 and SEP is in %

When examining the results of Figure 3, WV3 achieves a marginally better fit than S2 with S1 showing the poorest fit (R^2=0.51). In relation to the 1:1 trend line across all sensors (A-C), WV3 illustrated a closer fit especially between the 0-400 g/m^2 and around the 800 g/m^2 AGB range. All sensors, however, show signs of saturation from 700 g/m^2 AGB value which is indicative of noticeable AGB underestimation.

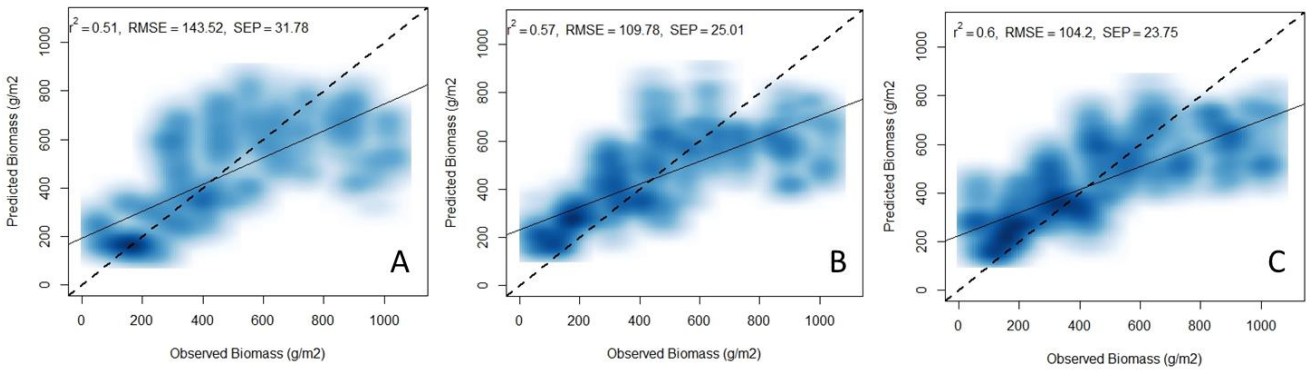

Figure 3: 100 Bootstrapped iterations, including accuracies, of observed versus predicted AGB density scatterplots derived from Sentinel-1 (A), Sentinel 2 (B) and WordView-3 (C) data only (dotted black line = 1:1 line).

According to Table 5, combining S1 polarisation channels and S2 reflectance bands, in particular, yielded higher accuracies than the use of these individual sensors alone and was also equivalent to the performance of the high resolution WV3 sensor

results (no significant difference between these scenarios with a p value of R^2 & RMSE > 0.05). Also the use of individual reflectance bands and polarisation channels generally yielded higher accuracies than the incorporation or use of VIs and band ratios with exception of the S1+S2 combination. The latter produced the best results and was used in creating the AGB maps. The LAI regional map, also required for the AGB map, was generated from the S2 dataset using the LAI PROSAIL RTM. Also the combination of either the S1 or S2 data with the high spatial resolution WV3 data did not yield any significant improvements in modelling accuracies compared to the combined S1 and S2 modelling results (p value of R^2 & RMSE > 0.05).

Table 5: Mean RF validation modelling results (of 100 bootstrapped iterations) for AGB prediction using a combination of the sensors in question

Scenarios	S1 + S2 (SAR + optical)			S1+WV3 (SAR + high res. optical)			S2+WV3 (optical + high res. optical)		
	R²	*RMSE*	*SEP*	*R²*	*RMSE*	*SEP*	*R²*	*RMSE*	*SEP*
Bands (Reflectance/ Polarisations)*	0.63	169.68	35.79	0.64	172.16	37.59	0.64	168.00	35.58
Indices (NDVIs/Band ratios)*	0.45	200.48	41.77	0.54	186.48	40.97	0.55	181.64	37.45
Band + Indices*	0.62	173.08	32.22	0.61	173.16	38.86	0.59	174.80	36.12

*Top 10 most important variables (LAI included in all scenarios); RMSE is in g/m^2 and SEP is in %

3.3 Predicted above ground biomass maps

Both AGB maps (figure 4) illustrated the expected patterning of high and low AGB throughout the study areas. In Hogsback, intermediate AGB ranges (320-560 g/m^2) were evident over the wetlands where stands of *T. capensis*, *P. australis* and *C. acutiformis* prevail (B-1). Lower AGB ranges (<320 g/m^2) were prevalent over the seasonally to temporary seep wetlands along slopes and Afromontane grassland areas (B-2). Pastoral fields mostly fell within this AGB range as well. The

Tevredenpan study area illustrated generally higher AGB ranges over the dryland HGM type compared to the Hogsback area (320-400 g/m^2 AGB range with less patches of AGB <240 g/m^2). Agricultural pastoral fields had typically a high AGB range (400-560 g/m^2) while similar ranges were found mostly along the valley-bottom wetlands (A-1). A few patches of high AGB (720-840 g/m^2) was found along the channels in the southern Pearl channelled valley-bottom wetland where the *Phr. australis* and *T. capensis* species were particularly dense (A-2). Interestingly, a high AGB value range (400-720 g/m^2) was also observed over the Tevredenpan, the very large depression in the south-western part of the study area, which consists of primarily floating *P. australis* in the centre surrounded by open water (A-3).

(A)

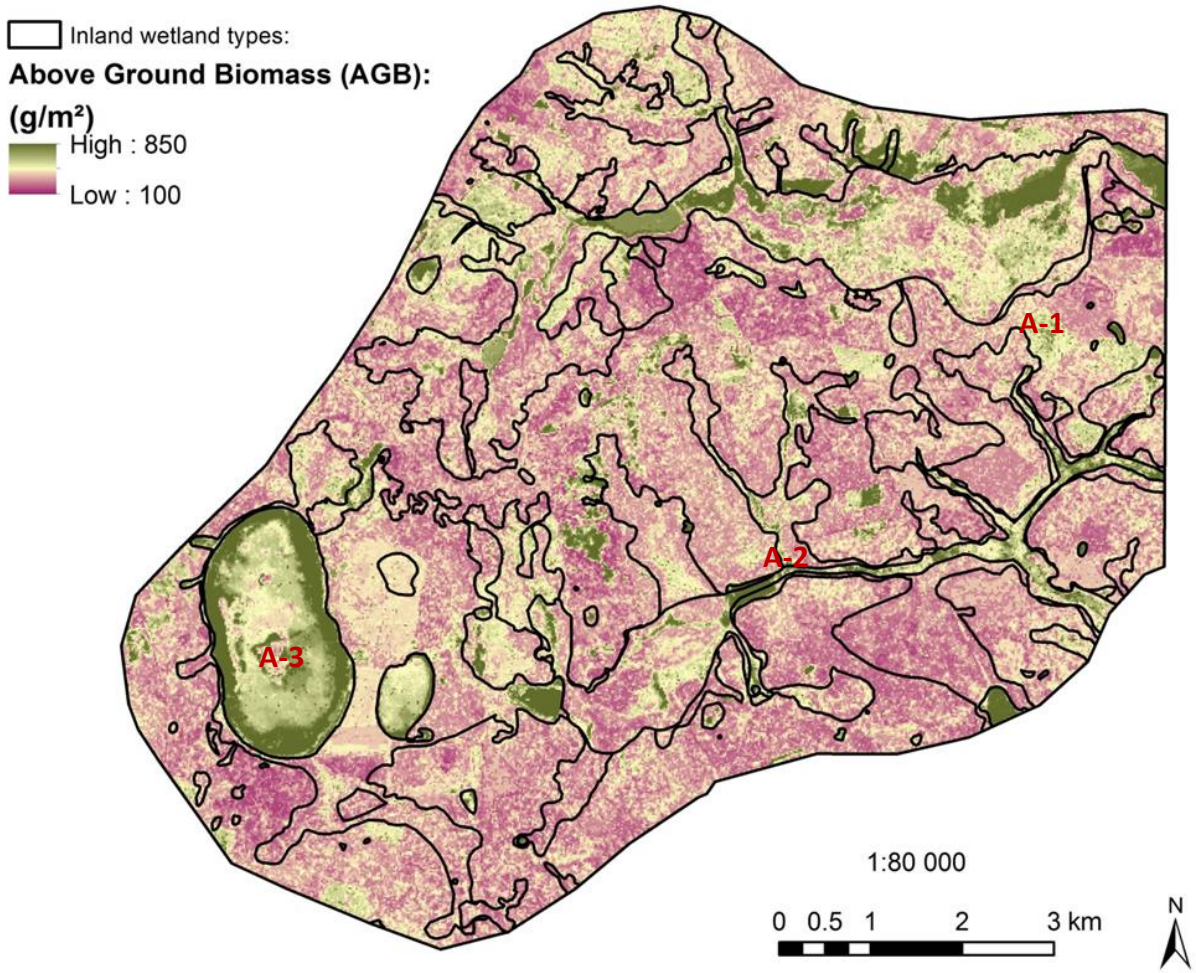

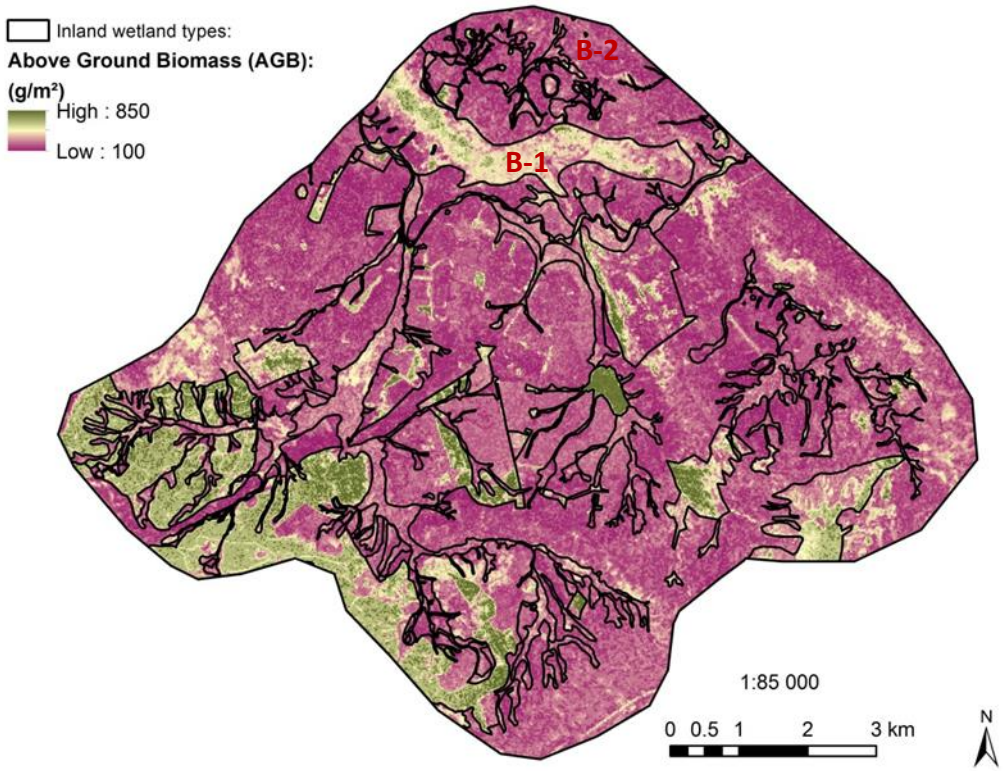

(B)

Figure 4: Above ground biomass (g/m^2) estimated from the combination of the Sentinel 1 (SAR) and 2 (optical) sensors for (A) Tevredenpan and (B) Hogsback.

3.4 Differences between wetland and dryland vegetation AGB

The mean AGB of wetlands was significantly higher ($p < 0.05$) than the dryland vegetation for both the ground samples and the predicted maps in both study sites (Figure 5, Table 6). Additionally, both ground samples and the predicted maps in Hogsback and Tevredenpan indicated a significant difference at the 99 percentile interval ($p > 0.001$) between wetland and dryland AGB (Table 6).

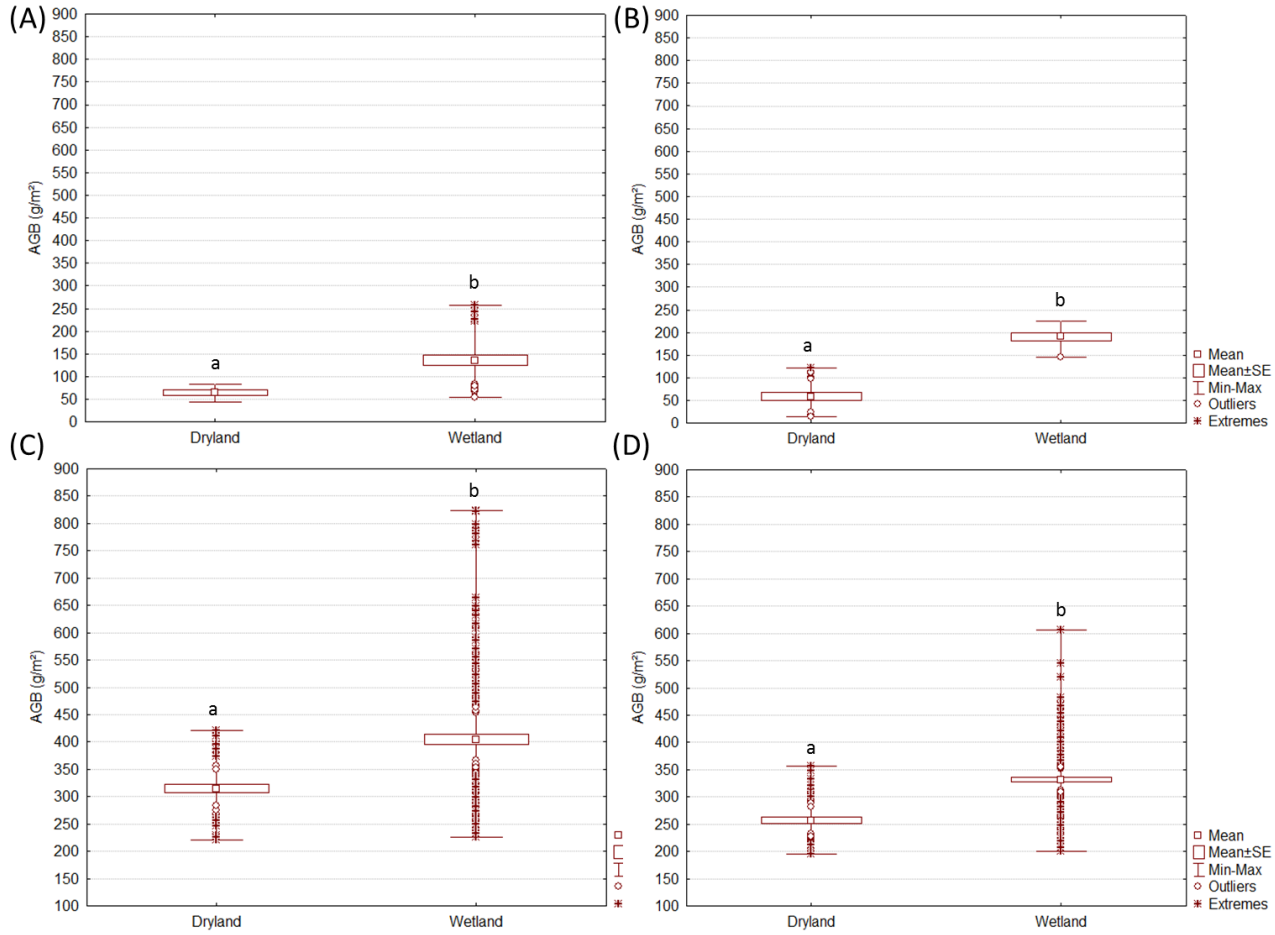

Figure 5: Variation in AGB across drylands and wetlands for (A) ground samples of Tevredenpan (Dryland *n* = 6, wetland *n* = 26); (B) the ground samples of Hogsback (Dryland *n* = 21; wetland *n* = 9) (C) the predicted AGB for Trevedenpan (Dryland *n* = 20, wetland *n* = 200); and (D) predicted AGB for Hogsback (Dryland *n* = 50, wetland *n* = 200); Significant differences between wetlands and drylands (t-test) are indicated in the letters below the boxplots

Table 6: Differences in AGB between wetlands and drylands (t-test, p < 0.05). The number of samples (n) is given for drylands, wetlands; df = degrees of freedom

	Ground samples			Predicted map		
	n	df	p	*n*	df	p
Tevredenpan	6, 26	29.5	0.0000134600000	50, 200	205.7	0.000000000004
Hogsback	21, 9	20.1	0.0000000009209	50, 200	120.2	0.0000000000000

Table 7: Statistics of predicted Above Ground Biomass (AGB) for drylands and wetland types of Tevredenpan and Hogsback

Predicted (g/m2)	Tevredenpan		Hogsback	
	Dryland	Wetland	Dryland	Wetland
Minimum	221.1	226.1	195.7	199.7
Mean	315	404.83	256.8	331.85
Maximum	421.3	823.2	356.5	605.9
Standard Deviation	52.9	38.16	42.1	10.97

COV	0.2	0.09	0.2	0.03

Based on the predicted AGB values per vegetation type (Table 7), it is evident that the Tevredenpan study site has a greater range of wetland vegetation than the Hogsback study site. These values range from a total range of 226.1 - 823.2 g/m^2 in comparison to the range of the more sedge-dominated Hogsback study site of 199.7 – 605.9 g/m^2. The Tevredenpan study site also possessed a slightly larger dryland AGB range with the mean values illustrating a difference of ~60 g/m^2.

3. Discussion

This study evaluated the capabilities of the Sentinel (1A and 2A) and WorldView-3 sensors for estimating herbaceous AGB, using Random Forest, in wetlands of two Afromontane study sites in the South African grassland biome. Additionally, the study sought to ascertain if there are significant differences in the AGB ranges between wetland vegetation and dryland vegetation types. Cost effective monitoring and quantification of AGB can improve the understanding of the functionality of plant material contribution to soil carbon sequestration at a regional scale in arid and semi-arid regions.

The modelling results indicated that the WV3 and Sentinel sensors can predict the AGB for two study areas and to the extent of dryland and wetland types. When the individual sensors were compared (WV3, S1 and S2), the WV3 sensor outperformed the other sensors attaining the highest coefficient of determination (R^2 = 0.63) and lowest RMSE and SEP (169.28 g/m^2 and ~35% respectively) using the WV3 individual bands in a RF model. WV offers a high spatial resolution (< 1m) and

498 although highly suited for modelling and monitoring AGB of wetlands in these arid to
499 semi-arid grasslands, the images are expensive for regional monitoring. Using a
500 combination of Sentinel SAR (S1) and optical (S2) with a spatial resolution of 20m
501 (aggregated to the coarser S1 spatial resolution), comparative results were obtained
502 using the individual bands and polarisations, attaining a coefficient of determination
503 of R^2 = 0.63 and an RMSE of 169.68 g/m^2 (SEP of ~ 36%) in a RF model. The
504 combination of the SAR and optical Sentinel sensors improved the modelling
505 performance over the use of the individual Sentinel sensors separately and were
506 comparable with accuracies obtained from the higher spatial resolution but more
507 expensive WV3 sensor. Huang et al. (2016), though predicted wetland AGB
508 including trees, also reported the benefit of integrating optical and SAR datasets.
509 This is due to volumetric (from the SAR sensor) and surface reflectance (with no risk
510 of saturation due to this study's AGB range) information being complementary and
511 when combined strengthened modelling performance. This result supports the idea
512 that wetland AGB can be suitably monitored with freely available satellite data albeit
513 at a coarser spatial resolution.
514
515 The intermediate modelling accuracies achieved in this study and the reliance on the
516 integration of LAI in the modelling procedure, however, could be linked to the field
517 sampling and data extraction protocol utilised in this study as in most cases, a single
518 S1 pixel and S2 pixel could have been extracted over each of the sample plots (the
519 field plots were smaller than the S1 and S2 pixels). Within the limited number of S1
520 and S2 pixels extracted, standing water and variable moisture presence between
521 wetland and dryland vegetation communities could have contributed as a source of
522 error in the modelling as both the S1 backscatter and S2 reflectance values would

523 have been affected. Mathieu et al., 2013, also, indicated that the use of a single pixel
524 of Radarsat-2 backscatter in woody vegetation modelling yielded poorer results in
525 comparison to more pixels aggregated from larger sampling windows. Additionally,
526 GPS error of the ground field plots and orthorectification of the S2 product could
527 have contributed to this error. Due to the heterogeneity of features (e.g. variable
528 hydrogeomorphic features between fine channel networks) associated with smaller
529 wetland systems, such as Hogsback and Tevredenpan, these sources of error would
530 be expected especially when utilising sensors of a 10-20m spatial resolution. In the
531 modelling results, the use of spectral indices and band ratios, unlike in the case of
532 Sibanda et al., 2017 and Mutanga et al., 2012, did not provide any improvements in
533 modelling accuracies in comparison to the use of reflectance and polarisation bands
534 alone. The lack of tonal variations (i.e. similar reflection, emittance, transmission or
535 absorption characteristics) between vegetation communities in these particular study
536 areas may support this result (Sibanda et al., 2017) but further investigation is
537 required.
538
539 The predicted AGB maps with an AGB range between 168-845 g/m^2, based on the
540 integrated Sentinel 1A and 2A RF model, was comparable and within the expected
541 range of other studies in palustrine wetlands of the grassland biome. Matayaya et
542 al., 2017 found several grass and sedge species associated with palustrine wetlands
543 of temperate grasslands north of Harare, Zimbabwe, to range from 92-2092 g/m^2 in
544 undisturbed sites. Li et al., 2017 documented a range of 122.31-1463.04 g/m^2 within
545 the temperate grassland study site in Inner Mongolia and Xie et al., 2009 obtained
546 mean ranges of up to 147g/m^2 in the same environment.
547

548 From the predicted maps, it was found that the predicted AGB values were
549 significantly different between wetland and dryland species. The AGB ranges within
550 these wetland and dryland vegetation types are controlled by the natural conditions
551 of such features (i.e. permanently and seasonally inundated) and disturbances from
552 the current land use practices (e.g. cattle grazing and fire). In the study area we
553 observed grazing in the temporary to seasonal seeps and valley-bottom wetlands of
554 both study areas, however seasonal saturation and inundation prohibits the
555 movement of cattle through certain wetland types. Some wetland vegetation, such as
556 the *P. australis*, *T. capensis* and *C. acutiformis*, are also not palatable, and hence
557 are less grazed. Regarding fire impacts, Matayaya et al., 2017, suggested the
558 presence of significantly lower AGB in areas where burning, clearing, clipping or
559 conventional tillage was applied but the impacts of fire in our study area were not
560 clearly visible. Thus, taking into account firstly the conditions of the hydroperiod and
561 secondly the impacts of grazing and fire, our results indicate that wetlands would
562 offer higher potential of maintaining expected ranges of AGB and carbon (i.e. higher)
563 relative to the drylands or temporary to seasonal seeps.
564
565 The estimation of AGB across dryland and wetland vegetation types can offer the
566 potential to monitor the functionality as well as pressures on wetlands over time.
567 Further studies should be done to determine the natural ranges (i.e. in the absence
568 of disturbances) of AGB for the dryland and wetland types, across the hydroperiod,
569 as a benchmark for functional intactness of wetlands in the landscape. It is also
570 unclear whether grazing and fire regimes impact all systems and to which degree as
571 the literature shows potential negative and positive impacts on soil nutrition, AGB

572 regrowth and species richness but ultimately, AGB is dependent on management
573 regimes of the area (Truus, 2011; Matayaya et al 2017).
574

575 ## 4. Conclusion

576 The paper assessed the capability of sensors to estimate above ground biomass
577 (AGB) of wetland vegetation in the grassland biome of South Africa. The combined
578 Sentinel SAR and optical sensors datasets achieved comparable results to the WV3
579 sensor, while being affordable for regional monitoring. Though being comparable,
580 WV3 still offers a greater spatial detail than the Sentinel sensors so the specific
581 applications will still dictate which sensor to use. The predicted AGB maps also
582 depicted an AGB range which was significantly different between wetland and
583 dryland grasses types. Estimation of the AGB of wetland vegetation enables carbon
584 sequestration studies and has the potential of monitoring functional intactness of
585 wetlands in the landscape.
586

587 ## Acknowledgements

588 This work was funded by the Water Research Commission (WRC) under the project
589 K5/2545 “Establishing remote sensing toolkits for monitoring freshwater ecosystems
590 under global change” as well as the Council for Scientific and Industrial Research
591 (CSIR) by the project titled “Common Multi-Domain Development Platform (CMDP)
592 to Realise National Value of the Sentinel Sensors for various land, freshwater and
593 marine societal benefit areas”. Thanks go to Mr Lufuno Vhengani from the Meraka
594 Institute at the Council for Scientific Research as well as Dr Clement Adjorlolo from
595 the South African National Space Agency (SANSA) who has supported the team

596 with the download and atmospheric correction of the Sentinel-2A images. To all the
597 land owners who graciously allowed access and assisted with local knowledge we
598 are most grateful, as well as Mr Chris Everton, Plantation Manager of, as well as the
599 land owners and the Amathole Forestry Company (Pty) Ltd for information on and
600 access to their property.

601

602

5. References

Amthor, J.S.; Dale, V.H.; Edwards, N.T.; Garten, C.T.; Gunderson, C.A.; Hanson, P.J.; Muston, M.A.; King, A.W.; Luxmoore, R.J.; McLaughlin, S.B.; Marland, G.; Muhlolland, P.J.; Norby, R.J.; O'Neill, R.V.; Post, W.M.; Shriner, D.S.; Rodd, D.E.; Tchaplinski, T.K.; Rurner, R.S.; Tuskan, G.A. and Wullschleger, S.D. 1998. Terrestrial ecosystem responses to global change: A research strategy, report, September 1, 1998; Tennessee. (digital.library.unt.edu/ark:/67531/metadc706583/: accessed August 2, 2018), University of North Texas Libraries, Digital Library, digital.library.unt.edu; crediting UNT Libraries Government Documents Department.

Amundson, R. 2001. The carbon budget in soils. Annual Review of Earth and Planetary Science. Vol 29; pp 535–562

Adam, E.; Mutanga, O.; Rugege, D. 2010. Multispectral and hyperspectral remote sensing for identification and mapping of wetland vegetation: a review. Wetlands Ecology and Management. 18; pp 281–296.

Burgoyne, B.M.; Bredenkamp, G.J.; van Rooyen, N. 2000. Wetland vegetation in the North-eastern Sandy Highveld, Mpumalanga, South Africa. Bothalia. 30 (2); pp 187-200

Cole, C.A. 2002. The assessment of herbaceous plant cover in wetlands as an indicator of function. Ecological Indicators, 2; pp 287 – 293.

Darvishzadeh, R.; Skidmore, A.K.; Schlerf, M.; Atzberger, C. 2008. Inversion of a radiative transfer model for estimating vegetation LAI and chorophyll in a heterogeneous grassland. Remote Sensing of Environment. 112(5); pp 2592-2604

Environmental Systems Research Institute (ESRI), 1999-2014

Fan, L.; Gao, Y.; Brück, H.; Bernhofer, C.H. 2009. Investigating the relationship between NDVI and LAI in semi-arid grassland in Inner Mongolia using in-situ measurements. Theoretical and Applied Climatology. 95; pp-151-156

Fourie, L.; Rouget, M.; Lötter, M. 2015. Landscape connectivity of the grassland biome in Mpumalanga, South Africa. Austral Ecology. 40; pp 67-76

Gallant, A.L. 2015. The challenges of remote monitoring of wetlands. Remote Sensing. 7; pp 10938-10950

GeoTerraImage (GTI) Pty Ltd. 2015. The 2013-2014 South African National Land-Cover Dataset, 2013-14 SA Landcover report-Contents vs 05 DEA open access. Data User Report and Metadata. Available: http://www.geoterraimage.com/downloads.php Accessed 17 September 2018.

Goudie and Wells, 1995. The nature, distribution and formation of pans in arid zone. Earth-Science Reviews. 38(1); pp 1-69

Grundling, P-L.; Linström, A.; Grobler, R.; and Engelbrecht, J. 2003. The Tevredenpan peatland complex of the Mpumalanga Lakes District. In: Couwenberg J and Joosten H (eds.) International Mire Conservation Group Newsletter Issue 2007/3. International Mire Conservation Group.

639 Huang, S.; Potter, C.; Crabtree, R.L.; Hager, S.; Gross, P. 2010. Fusing optical and radar data to
640 estimate sagebrush, herbaceous, and bar ground cover in Yellowstone. Remote Sensing of
641 Environment. 114; pp 251-264.

642 Huang, C.; Ye, Z.; Deng, C.; Zhang, Z.; Wan, Z. 2016. Mapping Above-Ground Biomass by Integrating
643 optical and SAR imagery: a case study of Xixi National Wetland Park, China. Remote sensing, 8, pp-1-
644 19

645 Intergovernmental Panel on Climate Change (IPCC). 2013. Working Group I Contribution to the IPCC
646 Fifth Assessment Report Climate Change 2013: The Physical Science Basis. Summary for Policy
647 makers. , pp. 1-36

648 Janks, M.R. 2014. Montane Wetlands of the South African Great Escarpment: Plant Communities and
649 Environmental Drivers. MSc thesis. Grahamstown, South Africa Rhodes University.

650 Jones, M.B. and Donnelly, A.; 2004. Carbon sequestration in temperate grassland ecosystems and
651 the influence of management, climate and elevated CO2. *New Phytologist*, 164 (3); pp 423 – 439

652 Kayranli, B. ; Scholz, M. ; Mustafa, Z. ; Hedmark, A. ; 2010. Carbon Storage and fluxes within
653 freshwater wetlands : a critical review. *Wetlands*. 30 ; pp 111 - 124.

654 Lal, R. 2008. Carbon sequestration. Philosophical Transactions of the Royal Society of Biological
655 Science. 363 (1492); pp 815–830.

656 Le Maitre, D.C.; Seyler, H.; Holland, M.; Smith-Adao, L.; Nel, J.L.; Maherry, A. and Witthüser. K. 2018.
657 Identification, Delineation and Importance of the Strategic Water Source Areas of South Africa,
658 Lesotho and Swaziland for Surface Water and Groundwater. Final Integrated Report on Project
659 K5/2431, Water Research Commission, Pretoria.

660 Lei, D.; Jingjuan, L.; Guazhuang, S. 2008. Neural network-based analytical model for biomass
661 estimation in Poyang Lake wetland using ENVISAT ASAR data. The International Archives of the
662 Photogrammetry, Remote Sensing and Spatial Information Sciences. Vol. XXXVII. Part B7. Beijing
663 2008; pp 1703 – 1708.

664 Li, Z.; Yeh, A. G-O.; Wang, S.; Liu, J.; Liu, X.; Qian, J.; Chen, X. 2007. Regression and analytical models
665 for estimating mangrove wetland biomass in South China using Radarsat images, International
666 Journal of Remote Sensing, 28:24, 5567-5582.

667 Liao, J.; Shen, G.; Dong, L. 2013. Biomass estimation of wetland vegetation in Poyang Lake area using
668 ENVISAT advanced synthetic aperture radar. Journal of Applied Remote Sensing, 7, pp 1-15.

669 Linström, A. 2015. Wetland Status Quo Report: Chrissiesmeer Project. Tevrede Pan Wetland W55A
670 (Wetlands W55A - 05 to 07). SANBI; Pretoria, South Africa.

671 MacKellar, N.; New, M.; Jack, C. 2014. Observed and modelled trends in rainfall and temperature for
672 South Africa: 1960-2010. South African Journal of Science - Climate trends in South Africa. 110(7/8);
673 pp 1-13

674 Masemola, C.; Cho, M.A.; Ramoelo, A. 2016. Comparison of Landsat 8 OLI and Landsat 7 ETM+ for
675 estimating grassland LAI using model inversion and spectral indices: case study of Mpumalanga,
676 South Africa. International Journal of Remote Sensing, 37(18); pp 4401-4419

677 Matayaya, G.; Wita, M.; and Nyamadzawo, G.; 2017. Effects of different disturbance regimes on
678 grass and herbacious plant diversity and biomass in Zimbabwean dambo systems. International
679 Journal of Biodiversity Science, Ecosystem Services and Management, 13(1); pp 181-190.

680 Mathieu, R.; Naidoo, L.; Cho, M.A.; Leblon, B.; Main, R.; Wessels, K.; Asner, G.P.; Buckley, J.; Van
681 Aardt, J.; Erasmus, B.F.N.; Smit, I.P.J. 2013. Toward structural assessment of semi-arid African
682 savannahs and woodlands: The potential of multitemporal polarimetric RADARSAT-2 fine beam
683 images. Remote Sensing of Environment, 138; pp 215-231

684 McDonald, J. H., 2008: Handbook of biological statistics. Baltimore: Sparky House Publishing.

685 Middleton, B.J. and Bailey, A.K. 2008. Water resources of South Africa, 2005 Study (WR2005) and
686 Book of Maps. WRC Research Reports No.TT381/08 & TT382/08.

687 Mitsch, W.J. and Gosselink, J.G. 2015. Wetlands. 5th ed. Hoboken (NJ): John Wiley & Sons.

688 Mpumalanga Tourism and Parks Agency (MTPA). 2014. Declaration of Chrissiesmeer Protected
689 Environment in terms of the Matopma; Environmental Management: Protected Areas Act, 2003 (Act
690 no 57 of 2003, as amended). Government Gazzette, 22 January 2014.

691 Mucina, L. and Rutherford, M.C. (2006). The Vegetation of South Africa, Lesotho and Swaziland.
692 Pretoria: South African National Biodiversity Institute (Strelizia)

693 Mueller-Wilm, U. 2017. Sentinel 2 MPC – Sen2Cor Configuration and User Manual. European Space
694 Agency (ESA); Issue 1; Date: 2018-03-22; pp 1-56

695 Mutanga, O.; Adam, E.; Cho, M.A. 2012. High density biomass estimation for wetland vegetation
696 using WorldView-2 imagery and random forest regression algorithm. International Journal of Applied
697 Earth Observation and Geoinformation. 18; pp 399-406

698 Nahlik, A.M. and Fennessy, M.S. 2016. Carbon storage in US wetlands. Nature Communications. 7
699 (13835); pp 1-9

700 Ollis, D.J.; Ewart-Smith, J.L.; Day, J.A.; Job, N.M.; Macfarlane, D.M.; Snaddon, C.D.; Sieben, E.J.J.; Dini,
701 J.A.; Mbona, N. 2015. The development of a classification system for inland aquatic ecosystems in
702 South Africa. Water SA. 41(5); pp 727 – 745.

703 Penuelas, J.; Gamon, J.A.; Griffin, K.L.; Field, C.B. 1993. Assessing community type, plant biomass,
704 pigment composition, and photosynthetic efficiency of aquatic vegetation from spectral reflectance.
705 Remote Sensing of Environment. 46; pp 110-118.

706 Republic of South Africa (RSA). 1998. National Water Act (NWA), Act 36 of 1998. Government
707 Printers: Pretoria, South Africa.

Poiani, K.A.; Johnson, W.C.; Kittel, T.G.F. 1995. Sensitivity of a prairie wetland to increased temperature and seasonal precipitation changes. Journal of the American Water Resources Association. 31(2); pp 283-294

Ramoelo, A.; Cho, M.A.; Mathieu, R.; Madonsela, S.; van de Kerchove, R.; Kaszta, Z.; Wolff, E. 2015. Monitoring grass nutrients and biomass as indicators of rangeland quality and quantity using random forest modelling and WorldView-2 data. International Journal of Applied Earth Observation and Geoinformation. 43; pp 43-54

Reid, H. and Huq, S. 2005. Climate change-biodiversity and livelihood impacts. Tropical Forests and Adaptation to Climate Change, p.57. https://books.google.co.za/books

Sibanda, M.; Mutanga, O.; Rouget, M. 2015. Examining the potential of Sentinel-2 MSI spectral resolution in quantifying above ground biomass across different fertilizer treatments. ISPRS Journal of Photogrammetry and Remote Sensing. 110; pp 55-65

Sibanda, M.; Mutanga, O.; Rouget, M.; Kumar, L. 2017. Estimating biomass of native grass grown under complex management treatments using WorldView-3 spectral derivatives. Remote Sensing. 9(55); pp 1-21

Sieben, E.J.J.; Mtshali, H.; Janks, M. 2014. National Wetland Vegetation Database: Classification and Analysis of wetland vegetation types for conservation planning and monitoring. Water Research Commission (WRC) Report No. 1980/1/14. WRC, Pretoria, South Africa.

Silva, T.S.F.; Costa, M.P.F.; Melack, J.M.; Novo, E.M.L.M. 2008. Remote sensing of aquatic vegetation theory and applications. Environmental Monitoring and Assessment. 140; pp 131-145

Sun, R.; Yao, P; Wang, W.; Yue, B.; Liu, G. 2017. Assessment of wetland ecosystem health in the Yangtze and Amazon River Basins. ISPRS International Journal of Geo-Information. 6(81); pp 1-14

Theuerkauf, S.J.; Puckett, B.J.; Theuerkauf, K.W.; Theuerkauf, E.J.; Eggleston, D.B. 2017. Density-dependent role of an invasive marsh grass, Phragmites australis, on ecosystem service provision. PLOS One. 12(2); pp 1-16

Truus L. 2011. Estimation of above ground biomass of wetland, biomass of wetland. In: Atazadeh I, edited. Biomass and Remote Sensing of Biomass. Shanghai: InTech; pp 75–86.

Turner, D.P.; Ollinger, S.V.; Kimball, J.S. 2004. Integrating remote sensing and ecosystem process models for landscape- to regional-scale analysis of the carbon cycle. BioScience. 54(6); pp 573-584

Ye, Y.; Zhou, C.; Sun, Y.; Zhou, D. 2010. Estimation of wetland aboveground biomass based on SAR Image: A case study of Honghe National Natural Reserve in Heilongjiang, China. 2010 18th International Conference on Geoinformatics, Beijing, China. 18-20 June 2010 (**ISBN:** 978-1-4244-7303-8)

Van Deventer, H.; Van Niekerk, L.; Adams, J.; Dinala, M.K.; Gangat, R.; Lamberth, S.J.; Lötter, M.; Mbona, N.; MacKay, F.; Nel, J.L.; Ramjukadh, C-L.; Skowno, A.; Weerts, S.P. submitted. National Wetland Map 5 – improving the spatial extent and representation of inland aquatic and estuarine ecosystems in South Africa.

Van Wijk, M.T.; Williams, M. 2005. Optical instruments for measuring leaf area index in low vegetation: application in artic ecosystems. Ecological Applications. 15(4); pp 1462-1470

Van Wilgen, N.J.; Goodall, V.; Holness, S.; Chown, S.L.; McGeoch, M.A. 2016. Rising temperatures and changing rainfall patterns in South Africa's national parks. International Journal of Climatology. 36(2); pp 706-721

Villa, J.A. and Mitch, W.J. 2015. Carbon sequestration in different wetland plant communities in the Big Cypress Swamp region of southwest Florida. International Journal of Biodiversity Science, Ecosystem Services & Management. 11(1); pp 17-28

Xie, Y.; Sha, Z.; Yu, M.; Bai, Y.; Zhang, L. 2009. A comparison of two models with Landsat data for estimating above ground grassland biomass in Inner Mongolia, China. Ecological Modelling, 220 (15), pp 1810-1818

Zedler, J.B. and Kercher, S. 2005. Wetland resources: status, trends, ecosystem services, and restorability. Annual Review of Environment and Resources. 30(1); pp 39-74